Introducing Condor: A High-Performance Array Telescope

Document 0001-A

February 2020

CONDOR

Contents

1 Introduction **4**

2 Background **4**

3 Configuration **5**
- 3.1 Telescopes . . . 6
- 3.2 Focal-Reducing Field Correctors . . . 6
- 3.3 CMOS Cameras . . . 6
- 3.4 Filter Wheels . . . 6
- 3.5 Focusers . . . 6
- 3.6 Mount . . . 6
- 3.7 Location . . . 7

4 Performance **7**
- 4.1 Plate Scale and Field of View . . . 8
- 4.2 Sensitivity . . . 8

5 Mode of Operation **9**

6 Scheduling and Software **9**

1 Introduction

The “Condor Array Telescope” or “Condor” is an “array telescope” that will consist of six 180 mm-diameter refracting telescopes—each equipped with a focal-reducing field corrector, large-format CMOS camera, motorized filter wheel, and motorized focuser—attached to a common robotic mount located in the Rio Hurtado Valley of Chile, among some of the best astronomical sites in the world. The telescope is funded by the Advanced Technologies and Instrumentation (ATI) program of the National Science Foundation (NSF) through the proposal “Concept Feasibility Study for a High-Performance Telescope Array,” which was awarded funding in August 2019 under NSF award number 1910001.

The research objectives of the project include (1) studying the low-surface-brightness outer regions of the Milky Way, the Large and Small Magellanic Clouds (LMC and SMC, respectively), and other nearby and distant galaxies and (2) studying transiting planets, gravitational microlensing events, and stars at a very rapid cadence of ≈ 60 s. The education and public outreach objectives of the project include (3) executing a far-reaching “broader impacts” program based on an allocation of 20% of the available observation time on the telescope, of which half of this 20% is specifically allocated to faculty and students at historically black colleges and universities (HBCUs).

The project is distinguished not only by the optical and mechanical properties of the telescope but also by the mode of operation of the telescope and the software infrastructure that supports the telescope. The project is explicitly a concept feasibility study for a much larger array telescope with much greater light-collecting capability.

As of February, 2020, the Condor Array Telescope is under construction and is expected to be deployed to Chile in the (Northern Hemisphere) summer of 2020. This document describes the conceptual design and expected configuration and capabilities of the telescope as of February 2020.

2 Background

Over the past several years, a new type of astronomical telescope known as a “telephoto array” or an “array telescope” has garnered significant scientific and popular attention. One aspect of the idea was pioneered by Abraham & van Dokkum [1], who combined eight off-the-shelf Canon telephoto lenses of focal length 400 mm and focal ratio $f/2.8$ (hence objective diameter 143 mm) with eight off-the-shelf CCD cameras and an off-the-shelf robotic telescope mount to form an eight-element “telephoto array,” which they named “Dragonfly.” The lenses that comprise Dragonfly are, of course, actually small *refracting* telescopes, which in contrast to *reflecting* telescopes are especially suitable to measuring low surface brightnesses. (Reflecting telescopes are ultimately limited in this regard by systematic effects caused by light that is diffracted by their secondary mirrors and then reflected and scattered by their optical assemblies.) Because Dragonfly is sensitive to low surface brightnesses, it has been able to discover a class of previously unknown “ultra-diffuse” galaxies, with sizes comparable to the size of the Milky Way but with only $0.1 - 1\%$ of the stars [11]. Dragonfly has also been used to demonstrate the lack of stellar halos around some spiral galaxies [10], to identify very low-surface-brightness companions of spiral [6] and elliptical [8] galaxies, and to study stellar halos of nearby galaxies [7]. Dragonfly is located in New Mexico in the Northern Hemisphere and has since been upgraded to 48 lenses.

And inspired by the success of Dragonfly, a group based at the Siding Spring Observatory in Australia is currently commissioning what amounts to a copy of the array (again using Canon telephoto lenses and CCD cameras), which they call “Huntsman” [5]. Because Huntsman is located in the Southern Hemisphere, about 500 km northwest of Sydney, it will be able to study regions of the sky that are inaccessible to Dragonfly. And indeed Dragonfly and Huntsman are themselves both inpired by previous array telescopes, many of which have been dedicated primarily to identifying transiting extra-solar planets. These include WASP [9], MASCARA [4], EVRYSCOPE [3], and others.

Considering the accomplishments of Dragonfly and the prospects of Huntsman, it became apparent to us that telescope arrays built from off-the-shelf refracting telescopes are indeed ideally suited to identifying and studying extremely low-surface-brightness galaxies and galaxy features. But we noted room for improvement in several important ways:

- Dragonfly is poorly suited to measuring point sources. The pixel scale of its detectors is very large (≈ 2.8 arcsec), hence point sources are typically undersampled and so susceptible to blending and intrapixel sensitivity variations [e.g. 2]. Further, the Canon lenses are not diffraction limited, hence point sources are blurred by the lenses themselves.

- The Canon lenses suffer significant vignetting, which limits possibilities of upgrading to larger-format detectors. Over the 18×14 mm^2 size of the Dragonfly detectors, Abraham & van Dokkum [1] measured vignetting at the field edge of 20%. But the “image circle” (i.e. the diameter over which the intensity exceeds 60% of the central intensity) of the lens is only ≈ 25 mm, and over a 36×24 mm^2 detector (a popular “full-frame” format for commercial detectors), the lens suffers vignetting at the field edge of 60%. Hence the lens can just barely illuminate a full-frame detector and certainly not a larger detector.

- Due to rapidly developing commercial CMOS technology, very large-format, very rapid-read-time, very low-read-noise cameras are just now becoming available. Whereas exposures with CCD cameras must be relatively long (typically ≈ 600 s) to maintain high duty cycle and remain sky-noise limited, exposures with these new CMOS cameras can be much shorter, offering for the first time the exciting possibility of observing the sky at a very rapid (say ≈ 60 s) cadence.

Our objective is to expand upon the pioneering work of previous array telescopes by building an array telescope optimized for detecting *both* extended, low-surface-brightness features *and* point sources and capable of efficiently imaging regions of the sky at an unprecedentedly rapid cadence of 60 s while remaining sky-noise limited.

These considerations led us to propose to the NSF ATI program building a high-performance array telescope located in the Southern Hemisphere, specifically in the Rio Hurtado Valley of Chile. The proposal was enthusiastically endorsed by the review panel, and the project was awarded funding. We dubbed this new array telescope the “Condor Array Telescope” or “Condor,” honoring its location in the Chilean Andes.

The low-surface-brightness sensitivity of Condor is relevant for studying the outer regions of the Milky Way, LMC, SMC, and other nearby and distant galaxies and for detecting ultra-diffuse galaxies in nearby clusters and in the field. The point-source sensitivity and rapid cadence of the array is relevant for studying transiting planets, gravitational microlensing events, and stars and gives high potential to yield unexpected discoveries.

3 Configuration

Here we describe the expected configuration of the telescope as of February 2020.

3.1 Telescopes

Condor will be based upon six Telescope Engineering Company (TEC) 180 mm-diameter f/7 refracting telescopes of focal length 1260 mm. The telescopes feature apochromatic, oil-spaced, triplet objective lenses with multi-layer coatings on all surfaces and a CaF_2 middle element.

3.2 Focal-Reducing Field Correctors

Each TEC telescope will be equipped with an Astro-Physics (AP) $0.72\times$ QUADTCC-TEC180 quad telecompressor corrector. This corrector used with the TEC 180 mm telescope yields an effective focal length of 907 mm and an effective focal ratio of f/5.0. The effective focal ratio of the six telescopes together, considered as a single instrument, is f/2.0.

3.3 CMOS Cameras

Each TEC telescope will be equipped with a ZWO ASI6200MM monochrome CMOS camera, which is based on the large-format Sony IMX455 back-illuminated sensor. Specifications of the CMOS cameras are summarized in Table 1.

Table 1: CMOS Camera Specifications

Sensor size	36×24 mm^2
Sensor format	9576×6388
Pixel size	3.76 μm
Maximum full-well capacity	51 ke$^-$
Read noise	1.3 to 3.5 e$^-$
ADC bits	16
Peak quantum efficiency	80%
Maximum full-resolution frame rate	3.2 fps

Various properties of the CMOS cameras, including the full-well capacity, gain, dynamic range, and read noise, are shown in Figure 1 as functions of gain setting. It is apparent from Figure 1 that there are obvious two choices of gain setting: A "low-gain" setting of 0 yields a full-well capacity of 51 ke$^-$, a read noise of 3.5 e$^-$, and a dynamic range of just under 14 stops, while a "high-gain" setting of 100 yields a full-well capacity of 19 ke$^-$, a read noise of 1.5 e$^-$, and a dynamic range of also just under 14 stops.

3.4 Filter Wheels

Each TEC telescope will be equipped with a ZWO EFW 7/2" seven-position filter wheel capable of holding 2-inch round filters.

3.5 Focusers

Each TEC telescope will be equipped with an Optec TCF-Leo low-profile motorized focuser.

3.6 Mount

The six TEC telescopes will be mounted onto a Planewave L-600 half-fork mount with equatorial wedge. The mount features direct-drive motors and precision encoders on each axis, slew speeds

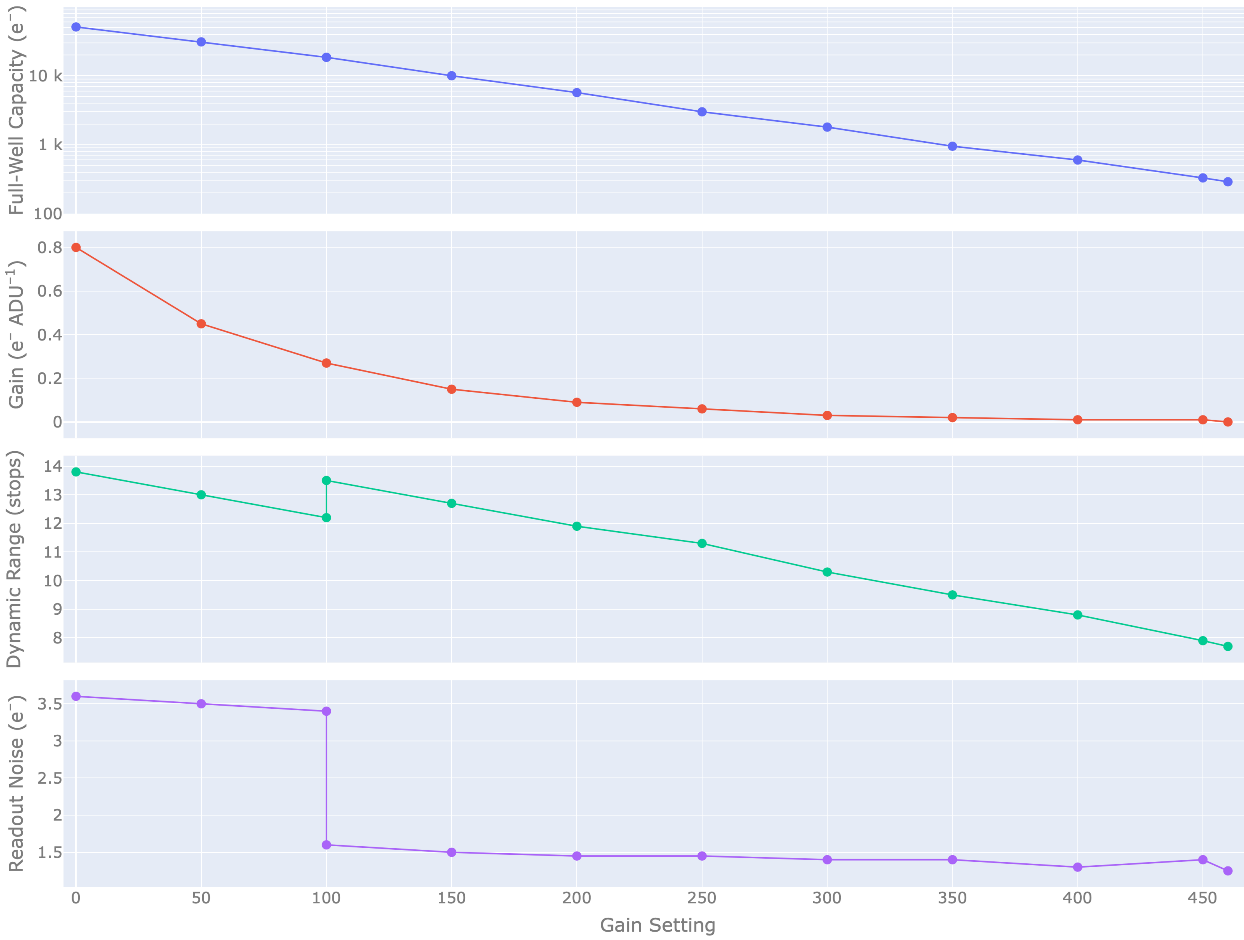

Figure 1: Various properties of the CMOS cameras, including the full-well capacity, gain, dynamic range, and read noise, as functions of gain setting.

of up to 50 deg s^{-1}, and zero backlash and periodic error. The telescopes will be attached to the mount using a bracket custom designed and fabricated by Optec. Various schematic representations of the six TEC telescopes (together with field corrector, CMOS camera, filter wheel, and focuser) and the Planewave mount are shown in Figure 3.

3.7 Location

The Condor Array Telescope telescope will be hosted at the El Sauce Observatory operated by Obstech in the Rio Hurtado Valley of Chile. The El Sauce Observatory is located around 27 km south of the Gemini telescope and LSST at Cerro Pachon, around 35 south of the Cerro Tololo Inter-American Observatory (CTIO) at Cerro Tololo, and around 138 km south of the La Silla Observatory operated by the European Southern Observatory.

4 Performance

Here we describe the expected performance of the telescope as of February 2020.

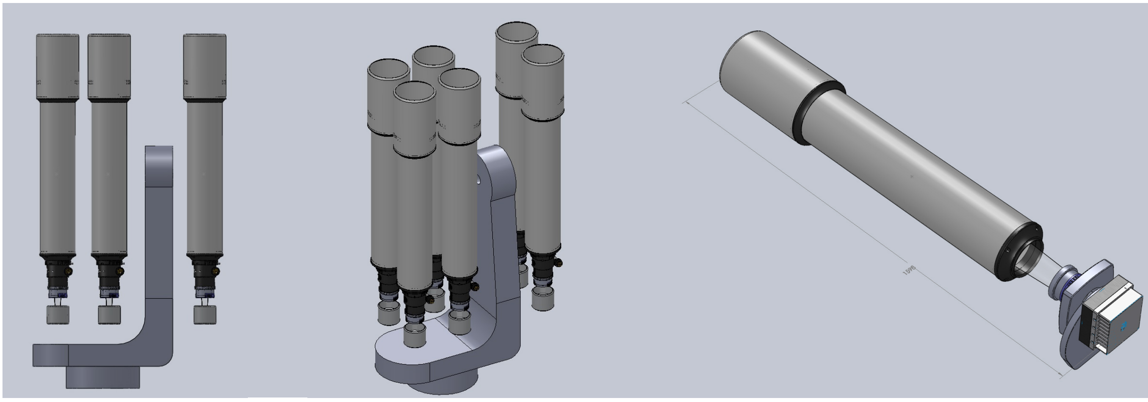

Figure 2: Schematic representations of the Condor Array Telescope, including six TEC telescopes configured onto a Planewave mount (left and middle) and one telescope configured with field corrector, CMOS camera, filter wheel, and focuser (right).

4.1 Plate Scale and Field of View

Considering the 3.76 μm pixel size of the 9576×6388 format Sony IMX455 sensor together with the effective focal length 907 mm of the TEC 180 mm telescope with the AP $0.72\times$ quad telecompressor corrector yields a plate scale of 0.86 arcsec pixel^{-1} and a field of view 2.3×1.5 deg^{-2}.

The Rayleigh limit of a 180 mm diameter aperture ranges from around 0.6 arcsec at B to around 1.0 arcsec at R, which when convolved with a seeing profile of, say, $\mathrm{FWHM} = 1.2$ arcsec typical of the El Sauce Observatory yields a point-spread function (PSF) of width ranging from $\mathrm{FHWM} \approx 1.3$ arcsec at B through $\mathrm{FWHM} \approx 1.6$ at R. The 0.86 arcsec pixel^{-1} plate scale of the telescope Nyquist samples a PSF of $\mathrm{FWHM} \approx 1.7$ arcsec, hence the telescope is expected to slightly undersample the PSF under seeing conditions typical of the El Sauce Observatory, by a factor ranging from as much ≈ 25% at B through as little as ≈ 7% at R.

4.2 Sensitivity

To predict performance of the telescope, we combined (1) the throughput of anti-reflection-multi-coated refracting optics, (2) the quantum efficiency versus wavelength curve of the Sony IMX455 sensor, and (3) the throughput of the atmosphere and the sky background appropriate to the Rio Hurtado Valley of Chile, estimated from the IRAF CCDTIME calculator for CTIO. (As described above, CTIO is only around 35 km from the El Sauce Observatory.) Resulting point-source and surface-brightness sensitivities of the array (including all six telescopes) over standard U, B, V, R, and I filters are summarized at various lunar phases in Table 2.

Noise contributions per 60 s exposure per individual telescope from sky noise and read noise per pixel and per point source are summarized in Table 3. At V, R, and I, a 60-s exposure is more or less sky-noise limited at all lunar phases. At B, a 60-s exposure is just barely sky-noise limited at lunar phase 0 d but more or less sky-noise limited beyond lunar phase 7 d. Hence the telescope is expected to satisfy our objective of efficiently imaging regions of the sky at an unprecedentedly rapid cadence of 60 s while remaining sky-noise limited.

Table 2: Point-Source and Surface-Brightness Sensitivities

	Point Source per 60 s (mag)			Surface Brightness per 30 h (mag arcsec^{-2})	Surface Brightness per 50 h (mag arcsec^{-2})
	Phase 0	Phase 7	Phase 14		
U ...	19.8	19.4	18.3	27.3	27.8
B ...	21.7	21.4	20.6	29.2	29.7
V ...	21.7	21.5	20.9	29.3	29.8
R ...	21.4	21.2	20.9	29.0	29.6
I	20.4	20.3	20.0	28.1	28.7

Note: Point source sensitivities are 5σ assuming a seeing $\mathrm{FWHM} = 1.2$ arcsec for lunar phase 0, 7, and 14 d. Surface-brightness sensitivities are 3σ averaged over 10×10 arcsec^2 regions of the sky and lunar cycle.

Table 3: Noise Contributions per 60 s Exposure

	Per Point Source						Per Pixel					
	Phase 0		Phase 7		Phase 14		Phase 0		Phase 7		Phase 14	
	Sky	Read	Sky	Read	Sky	Read	Sky	Read	Sky	Read	Sky	Read
U ...	1.4	2.4	3.9	2.4	15.5	2.4	0.9	1.5	2.5	1.5	9.8	1.5
B ...	2.8	2.4	4.7	2.4	12.5	2.4	1.7	1.5	2.9	1.5	7.7	1.5
V ...	5.1	2.5	6.5	2.5	12.0	2.5	3.0	1.5	3.8	1.5	7.1	1.5
R ...	8.5	2.7	9.8	2.7	13.5	2.7	4.8	1.5	5.5	1.5	7.6	1.5
I	9.5	2.9	7.6	2.9	13.4	2.9	5.0	1.5	5.5	1.5	7.0	1.5

Note: Noise contributions per 60 s exposure per individual telescope from sky noise and read noise per point source and per pixel are in units of e$^-$ and are presented for lunar phase 0, 7, and 14 d. Noise contributions per point source assume a seeing $\mathrm{FWHM} = 1.2$ arcsec.

5 Mode of Operation

In its normal mode of operation, we expect the telescope to obtain deep images by combining many 60 s exposures acquired over intervals spanning many tens of hours. Because the read time of the cameras is less than 1 s, the duty cycle will be nearly 100%. And because the read noise of the cameras is only ≈ 1.5 e$^-$, each exposure will be sky-noise limited ,as described above. In this way, the telescope will *simultaneously* build up images of low-surface-brightness sensitivity *and* monitor point sources at an unprecedentedly rapid cadence of 60 s while remaining sky-noise limited.

6 Scheduling and Software

The telescope will be equipped with a new software infrastructure that allows access to be allocated on either a per-observation or a per-hour basis via a "credit" system. By issuing credits—to researchers, educators, and public outreach institutions—access to the telescope can be shared in a very flexible way. As examples: a researcher might use credits to obtain observations to assess feasibility of a project prior to writing a proposal; an educator might use credits to let students obtain observations for an observational astronomy laboratory course; and a science museum lecturer might use credits to show celestial objects to an audience following a public seminar. We dub this capability "Elastic Cloud Astronomy," in direct analogy with AWS Elastic Cloud Computing by Amazon.

References

[1] R. G. Abraham and P. G. van Dokkum. Ultra-Low Surface Brightness Imaging with the Dragonfly Telephoto Array. *PASP*, 126:55–69, 2014.

[2] D. Kavaldjiev and Z. Ninkov. Effects of Sub-Pixel Sensitivity Variations. *Optical Engineering*, 40:162, 2001.

[3] N. M. Law, O. Fors, J. Ratzloff, P. Wulfken, D. Kavanaugh, D. J. Sitar, Z. Pruett, M. N. Birchard, B. N. Barlow, K. Cannon, S. B. Cenko, B. Dunlap, A. Kraus, and T. J. Maccarone. Evryscope Science: Exploring the Potential of All-Sky Gigapixel-Scale Telescopes. *PASP*, 127:234, March 2015.

[4] A.-L. Lesage, J. F. P. Spronck, R. Stuik, F. Bettonvil, D. Pollaco, and I. A. G. Snellen. MASCARA: the multi-site all-sky CAameRA: concept and first results. In Larry M. Stepp, Roberto Gilmozzi, and Helen J. Hall, editors, *Ground-based and Airborne Telescopes V*, volume 9145, pages 402 – 409. International Society for Optics and Photonics, SPIE, 2014.

[5] F. Longbottom. Ultra faint imaging with the Huntsman Telescope. In *Linking Galaxies from the Epoch of Initial Star Formation to Today*, page 82, February 2019.

[6] A. Merritt, P. van Dokkum, and R. Abraham. The Discovery of Seven Extremely Low Surface Brightness Galaxies in the Field of the Nearby Spiral Galaxy M101. *ApJ*, 787:L37, June 2014.

[7] A. Merritt, P. van Dokkum, R. Abraham, and J. Zhang. The Dragonfly nearby Galaxies Survey. I. Substantial Variation in the Diffuse Stellar Halos around Spiral Galaxies. *ApJ*, 830:62, October 2016.

[8] A. Merritt, P. van Dokkum, S. Danieli, R. Abraham, J. Zhang, I. D. Karachentsev, and L. N. Makarova. The Dragonfly Nearby Galaxies Survey. II. Ultra-Diffuse Galaxies near the Elliptical Galaxy NGC 5485. *ApJ*, 833:168, December 2016.

[9] D. L. Pollacco, I. Skillen, A. Collier Cameron, D. J. Christian, C. Hellier, J. Irwin, T. A. Lister, R. A. Street, R. G. West, D. R. Anderson, W. I. Clarkson, H. Deeg, B. Enoch, A. Evans, A. Fitzsimmons, C. A. Haswell, S. Hodgkin, K. Horne, S. R. Kane, F. P. Keenan, P. F. L. Maxted, A. J. Norton, J. Osborne, N. R. Parley, R. S. I. Ryans, B. Smalley, P. J. Wheatley, and D. M. Wilson. The WASP Project and the SuperWASP Cameras. *PASP*, 118(848):1407–1418, Oct 2006.

[10] P. G. van Dokkum, R. Abraham, and A. Merritt. First Results from the Dragonfly Telephoto Array: The Apparent Lack of a Stellar Halo in the Massive Spiral Galaxy M101. *ApJ*, 782:L24, February 2014.

[11] P. G. van Dokkum, R. Abraham, A. Merritt, J. Zhang, M. Geha, and C. Conroy. Forty-seven Milky Way-sized, Extremely Diffuse Galaxies in the Coma Cluster. *ApJ*, 798:L45, January 2015.